Creep in Colloidal Glasses

M. Siebenbürger,[1] M. Ballauff,[1] and Th. Voigtmann[2,3]

[1]*Helmholtz-Zentrum für Materialien und Energie, 14109 Berlin, Germany*
[2]*Institut für Materialphysik im Weltraum, Deutsches Zentrum für Luft- und Raumfahrt (DLR), 51170 Köln, Germany*
[3]*Zukunftskolleg and Fachbereich Physik, Universität Konstanz, 78457 Konstanz, Germany*
(Received 3 April 2012; published 18 June 2012)

We investigate the nonlinear response to shear stress of a colloidal hard-sphere glass, identifying several regimes depending on time, sample age, and the magnitude of applied stress. This emphasizes a connection between stress-imposed deformation of soft and hard matter, in particular, colloidal and metallic systems. A generalized Maxwell model rationalizes logarithmic creep for long times and low stresses. We identify diverging time scales approaching a critical yield stress. At intermediate times, strong aging effects are seen, which we link to a stress overshoot seen in stress-strain curves.

The nonlinear response of amorphous solids to external forces challenges our understanding of slow structural dynamics and the mechanisms of solid formation. Under sustained load, a solid deforms viscoplastically and may eventually yield to flow or fail otherwise. The resulting slow deformation called creep has been investigated for over a century [1,2] and can be a major concern in engineering applications. It is known from hard-condensed matter such as metals, window glasses, and rocks [3,4], and, more recently, from a variety of amorphous soft matter [5–10]. This calls for a more detailed analysis of universal aspects of creep in hard and soft matter, and how to link various nonlinear material properties probed under applied load or applied deformation rate.

Here we report on the creep in well-characterized hard-sphere-like colloidal suspensions close to the glass transition, imposing a fixed shear stress σ after aging the shear-molten initial stage for various waiting times t_w. Monitoring the deformation $\gamma(t)$ over much larger time spans than usual, we uncover several regimes in the slow structural dynamics. We link a nontrivial age dependence to nonmonotonic local stress relaxation. Close to the yield stress σ_c (distinguishing solidlike deformation from plastic flow), we identify a diverging time scale connected to low-stress logarithmic creep.

Soft-matter creep has been discussed in the soft glassy rheology (SGR) [11], fluidity models [10,12], or in terms of time-dependent structural changes [6]. We follow a generic route based on a recent nonlinear-response formalism [13,14]. Ignoring tensorial aspects for simplicity,

$$\sigma(t) = \int_{-\infty}^{t} \dot{\gamma}(t') G(t, t', [\dot{\gamma}]) dt'. \quad (1)$$

The dynamical shear modulus G depends on 2 times separately outside stationary states, and on the shear-rate history in nonlinear response. The linear Maxwell model for viscoelastic fluids [4] sets $G(t - t') = G_\infty \exp[-(t - t')/\tau]$ where G_∞ is the low-frequency (plateau) shear modulus, and τ a structural relaxation time. Strong shear ($\dot{\gamma}\tau \gg 1$)

typically causes shear thinning by accelerated structural relaxation (directly observed in colloids [15]), requiring G to depend on $\dot{\gamma}$. We are concerned with determining those $\dot{\gamma}(t)$ that fulfill Eq. (1) for a given constant σ. The existence of unique inversions of such a nonlinear integral equation is nontrivial, and will be assumed here. To highlight generic features of creep, we discuss the consequences of Eq. (1) separately for various time windows, from elastic to plastic deformation regimes.

Experiments are performed on core-shell PS-PNIPAM particles with a solid poly(styrene) core and a shell of poly(N-isopropylacrylamide) with 2.5 mol% N,N'-methylenebisacrylamide (BIS) crosslinker, synthesized and purified as in Ref. [16]. Suspension in an aqueous 5×10^{-2} mol/l KCl solution screens electrostatic interactions and makes the system a model for hard spheres [17]. Particles are polydisperse in size (17%) and thermosensitive; below 25°C their hydrodynamic radius follows $R[\text{nm}] \approx 102.4096 \, \text{nm} - 0.7796T \, \text{nm}/°\text{C}$ [17]. We use two batches of suspensions: (A) (8.37 ± 0.02) wt% at $T = (15 \pm 0.05)°\text{C}$; (B) (7.99 ± 0.02) wt% at $T = (12 \pm 0.05)°\text{C}$. Within error bars, the effective volume fractions are equal (verified by steady-state flow curves, which are identical), $\varphi = 0.65 \pm 0.02$ and $\varphi = 0.67 \pm 0.02$, respectively. The glass transition is at $\varphi_c \approx 0.64$ [17].

We use a stress-controlled rotational rheometer MCR 301 (Anton Paar) with a cone-plate system (diameter: 50 mm, cone angle: 0.991°, gap height: 0.053 mm). Sealing the gap with a thin film of low-viscosity parafine oil minimizes solvent evaporation. Preshear ($\dot{\gamma} = 100/\text{s}$) was applied for 200 s, followed by a waiting time t_w.

Reduced units emphasize the expected generality of the results: $k_B T/R^3 \approx 5.5$ Pa for stresses, and $\tau_0 = R^2/D_0 \approx 0.004(1)$ s for times (D_0 is the free diffusion coefficient). Our system is characterized by a nonvanishing dynamic yield stress $\sigma_y \approx 0.4 kT/R^3$ [17].

Figure 1 shows the central result of the creep experiment: the time-dependent strain and strain rates following
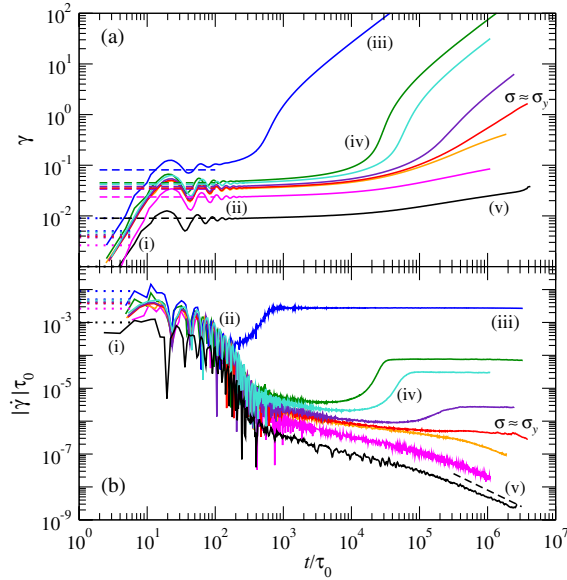
FIG. 1 (color online). (a) Deformation $\gamma(t)$ after application of a fixed stress $\hat{\sigma} = \sigma/(k_B T/R^3) = 0.9$, 0.5, 0.4693, 0.4224, 0.3943, 0.3755, 0.2628, and 0.1 (top to bottom: all batch A except $\hat{\sigma} = 0.9$, 0.5, 0.1); waiting time $t_w = 600$ s. Dotted (dashed) lines: short-time (glass-modulus) elastic response. Labels (i) to (v) mark regions discussed in the text. (b) Shear rate $\dot{\gamma}(t)$ obtained from differentiating the measured $\gamma(t)$ (smoothened for $\sigma = 0.1$). Dotted lines: $\delta\dot{\gamma}(0)$, see text. Dashed line: $\dot{\gamma} \propto t^{-1}$.

the application of constant stress σ at $t = 0$, for various σ and a waiting time $t_w = 600$ s $\approx 1.3 \times 10^5 \tau_0$. Our measurements extend previous ones for similar systems [18–20] to larger time spans and larger t_w/τ_0 (see below). Some of the measurements around the yield stress have been repeated (not shown), to ensure reproducibility. The data exhibit five regimes. (i) An initial fast growth in $\gamma(t)$ followed by oscillations. The latter have been associated with rheometer inertia [21,22] and will not be analyzed here. (ii) After that, $\gamma(t)$ shows a plateau over a time window that expands if σ is lowered. The height of this plateau depends linearly on σ, indicating elastic response. (iii) At large stresses, $\sigma > \sigma_c$, and long times, viscous flow occurs, characterized by a constant $\dot{\gamma}(\sigma)$. None of these regimes depend on aging. (iv) Before entering viscous flow, a superlinear increase in $\gamma(t)$ follows the plateau, sometimes identified with sudden "breaking" [23,24]. For $\sigma < \sigma_c$, a power law $\dot{\gamma}(t) \sim t^{-x}$ is indicated. This regime shows strong age dependence, discussed below. (v) At small stresses, $\sigma < \sigma_c$, shear rates continue to decay indefinitely for experimentally accessible times. The data are compatible with $\dot{\gamma}(t) \sim 1/t$ (indicated by a dashed line) at the longest times, revealed by a constant in $\dot{\gamma}t$ (not shown).

Let us rationalize the five regimes using Eq. (1). A stress σ imposed as an ideal step at $t = 0$ causes an instantaneous elastic strain γ_0: $\dot{\gamma}(t) = \gamma_0 \delta(t) + \delta\dot{\gamma}(t)$ where $\delta(t)$ is the Dirac delta. The delayed strain rate $\delta\dot{\gamma}(t)$ is regular for $t \to 0$ and vanishes for $t < 0$ due to causality, so that

$$\sigma = \gamma_0 G(t, 0, [\dot{\gamma}]) + \int_0^t \delta\dot{\gamma}(t') G(t, t', [\delta\dot{\gamma}])dt', \quad (2)$$

$\gamma_0/\sigma = 1/G_0$, with the high-frequency shear modulus G_0. Independent linear-response measurements [17] give $G_0 \approx 100 k_B T/R^3$ for our system; corresponding γ_0 are indicated in Fig. 1(a) (dotted lines).

Differentiation of Eq. (2) for $t \to 0$ determines the initial delayed deformation rate $\delta\dot{\gamma}_0$. Estimating the short-time relaxation rate of the modulus as $\dot{G}_0 = (d/dt)G(t, t')_{t' \to t} \sim -G_0/\tau_0$, we get $\delta\dot{\gamma}_0 \tau_0 \sim \sigma/G_0$ [dotted lines in Fig. 1(b)]. The values are compatible with the measured $\dot{\gamma}$ at short times, regime (i), and serve as an upper bound expected from linear response.

In the quiescent ideal glass, $G(t, t')$ attains a long-time limit $G_\infty < G_0$, the low-frequency (Maxwell) modulus. Equation (2) then predicts the linear deformation of the glass, $\delta\gamma \sim \gamma_0(G_0 - G_\infty)/G_\infty$. For hard-sphere–like systems $G_\infty/G_0 \approx 1/10$ [25], so that $\delta\gamma = \mathcal{O}(10)\gamma_0$. These values [dashed lines in Fig. 1(a)] agree well with the measurement in regime (ii). Subsequent plastic deformation is then caused by the long-time structural dynamics (α relaxation in the nomenclature of glassy dynamics).

In the viscous-flow regime (iii), $\sigma > \sigma_c$, the flow rate $\dot{\gamma}(\sigma)$ is constant and, within experimental error, given by the flow curve $\sigma(\dot{\gamma})$ obtained from rate-controlled steady-state rheology, see Fig. 2. In principle, the static yield stress, σ_c, could differ from the dynamic one, σ_y, obtained from a sequence of steady-state rate-driven flows with $\dot{\gamma} \to 0$. Molecular dynamics simulations of glassy dynamics found $\sigma_c \approx 1.2\sigma_y$ [26]. Our experiments cannot distinguish between the two, $\sigma_c \approx \sigma_y \approx 0.4 k_B T/R^3$.
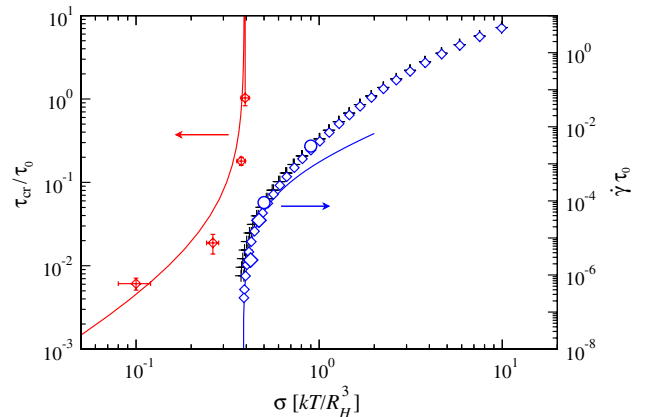
FIG. 2 (color online). Steady-state flow curve $\dot{\gamma}(\sigma)$ (right axis) from constant-rate experiments in increasing and decreasing sequence (crosses; $t_w = 10$ s), and from the stress-controlled mode of the rheometer (small diamonds). Values read off from Fig. 1 are shown as large diamonds and circles (batches A and B). Solid line: Herschel-Bulkley law, $\sigma - \sigma_c \propto \dot{\gamma}^n$, with $1/n \approx 1.85$, $\sigma_c \approx 0.38$. Left axis: time scale τ_{cr} for logarithmic creep from the data (symbols) and a generalized Maxwell model (line), see text.

The time scale for the crossover to viscous flow increases as σ_c is approached from above. This follows from Eq. (2) since the steady-state $G(t)$ decays on a time scale $t_f \sim 1/\dot{\gamma}(\sigma)$. Since the flow curve can be fitted with a (Herschel-Bulkley) power law (see Fig. 2), $\sigma(\dot{\gamma}) - \sigma_c \propto \dot{\gamma}^n$ close to σ_c, the fluidization time t_f diverges as $(\sigma(\dot{\gamma}) - \sigma_c)^{-1/n}$. For our system, $1/n \approx 1.85$. This divergent time scale has also been identified recently [9]. The value of $1/n$ depends on the fitting region; we take the power law to be an asymptotic expression for $\sigma \to \sigma_c$, as expected from theory [27]. Right at the yield stress, sublinear rise in $\gamma(t)$ is expected to continue indefinitely: the curves closest to σ_y in Fig. 1 exemplify this. It has been suggested that a minimum shear rate for steady flow exists [28]; indeed, $\dot{\gamma}\tau_0 \gtrsim 5 \times 10^{-7}$ holds for those $\sigma > \sigma_y$ we could measure.

We now examine the waiting-time dependent regime (iv). Combining the once and twice differentiated Eq. (1),

$$\delta\ddot{\gamma}(t) = \int_{-\infty}^{t} \dot{\gamma}(t')\left[\partial_t G(t,t')\frac{\dot{G}_0}{G_0} - \partial_t^2 G(t,t')\right]dt'. \quad (3)$$

For linear-response colloidal dynamics, one proves that autocorrelation functions such as $G(t - t')$ are completely monotone [29]: $(-d/dt)^n G(t) \geq 0$ for all integer $n \geq 0$. Assuming $G(t, t')$ to be completely monotone in t for every t', Eq. (3) yields $\delta\ddot{\gamma}(t) \leq 0$ for all $t > 0$ [30]. This inequality is not obeyed for superlinear creep.

$G(t, t')$ that violate complete monotonicity are known from rate-controlled startup experiments, where a constant $\dot{\gamma}_{so}$ is switched on at $t = 0$: typically the resulting stress $\sigma(t)$ exhibits a maximum σ_{max} at the end of the initial elastic regime before decreasing to its steady-state value [4]. From Eq. (1), this stress overshoot implies a negative dip in the corresponding $G(t - t', \dot{\gamma}_{so})$ [25,31]. Our model system also exhibits stress overshoots, cf. Fig. 3: at the strain rates considered, σ_{max} is reached for $\dot{\gamma}_{so}t \approx 0.1$, indicating a typical strain for yielding of nearest-neighbor cages [31].

Both the stress overshoot and the superlinear creep regime show significant age dependence. This is highlighted in Fig. 3 by curves for $t_w = 60, 600, 3600,$ and 6000 s ($t_w/\tau_0 = 1.3 \times 10^4$, 1.3×10^5, 7.5×10^5, and 1.3×10^6). The same waiting times have been used in the creep experiment; results are shown in Fig. 4. The height of the overshoot σ_{max} increases with increasing t_w while the initial elastic and final viscous parts of the stress-strain curve do not change. As previously reported [26,32], the ratio $r = (\sigma_{max} - \sigma(\dot{\gamma}))/\sigma(\dot{\gamma})$ [Fig. 3(b), open symbols] grows logarithmically for two decades of waiting time. To compensate for this growth, the accumulated strain needs to decrease at intermediate times. Indeed, for the creep experiment, $r' = 1/(G_\infty\dot{\gamma}_{min}\tau_f)$ grows roughly logarithmically with t_w (filled symbols). Here, $\dot{\gamma}_{min}$ is the minimum of the creep shear rate [cf. Fig. 4(b)], and τ_f is the time where $\dot{\gamma}$ rises again [estimated from $\gamma(\tau_f) = 0.2$
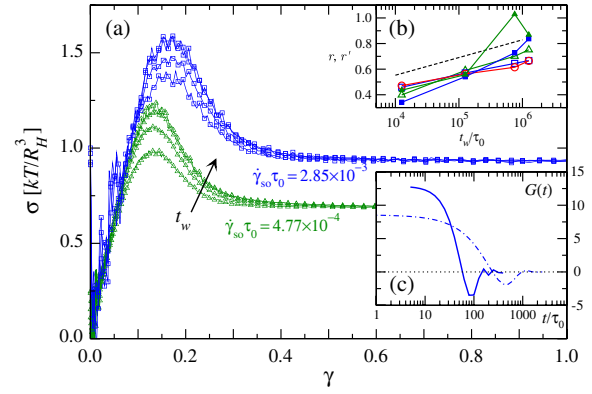
FIG. 3 (color online). (a) Stress-strain curves: Startup stress $\sigma(t)$ at constant shear rate $\dot{\gamma}_{so}$ (symbols with lines, batch B), as a function of strain $\gamma = \dot{\gamma}_{so}t$ after switch-on, waiting times as in Fig. 4. (b) Ratio $r = \sigma_{max}/\sigma(\dot{\gamma}) - 1$ (open symbols) and $r' = 1/(G_\infty\dot{\gamma}_{min}\tau_f)$ from the creep experiment (filled) as a function of t_w; see text. Dashed line: $0.06 \ln t_w/\tau_0$. (c) Shear modulus $G(t)$ for $\dot{\gamma}_{so}\tau_0 = 2.85 \times 10^{-3}$ and $t_w = 6000$ s (solid line), and from $\gamma(t)$ (dash-dotted in Fig. 4) and the convolution approximation.

in Fig. 4(a)]. As evidenced in Fig. 4(b), $\dot{\gamma}_{min}$ indeed decreases with increasing sample age.

It is therefore plausible that related mechanisms lead to the stress overshoot and to superlinear creep. A simple ansatz allows us to understand such connection. Approximating Eq. (1) as a convolution, the Laplace transform reads $\sigma/s = s\gamma(s)G_{creep}(s)$. Assuming $\dot{\gamma}(t)$ to be a combination of three constant shear rates [$\delta\dot{\gamma}_0$, $\dot{\gamma}_{min}$, and $\dot{\gamma}(\sigma)$], cf. the dash-dotted line in Fig. 4, the convolution approximation estimates $G_{creep}(t)$ as shown in Fig. 3(c) (dash-dotted line). It indeed displays relaxation involving a negative dip typical for the overshoot dynamics, $G_{so}(t)$ [solid line in Fig. 3(c), from $\partial_t\sigma_{so}(t)$]. $G_{creep}(t)$ decays about 4 times slower than $G_{so}(t)$; this is expected since in the relevant time window, the shear rate entering $G_{creep}(t)$ is still roughly $\dot{\gamma}_{min}$. From Fig. 4, we indeed estimate $1/\dot{\gamma}_{min} \approx 4 \times 1/\dot{\gamma}(\sigma)$ for the relevant time scales. Recall that $G(t)$ is a microscopic stress-stress autocorrelation function. The physical mechanism leading to the dip is thus identified as an "elastic recoil": local stresses overrelax when nearest-neighbor cages break under external driving [31,33].

For $\sigma < \sigma_y$, Eq. (1) can only be solved by an asymptotically decreasing $\delta\dot{\gamma}(t)$. Regime (iv) here suggests a power law, $\dot{\gamma}(t) \approx t^{-x}$. This may be just a crossover phenomenon. Yet, a power law with $x = 2/3$ has been suggested for creep in metal wires by Andrade already in 1910 [2]; it is called β creep in hard-condensed matter, and has recently been found in paper and soft-matter gels [8,9]. A dash-dotted line in Fig. 4 shows the Andrade creep law for comparison. Derivations of β creep are based on dislocation dynamics [34–36] and hence not easily transferred to amorphous systems. Although not confirmed by a rigorous argument, one possibility is the critical decay law of the
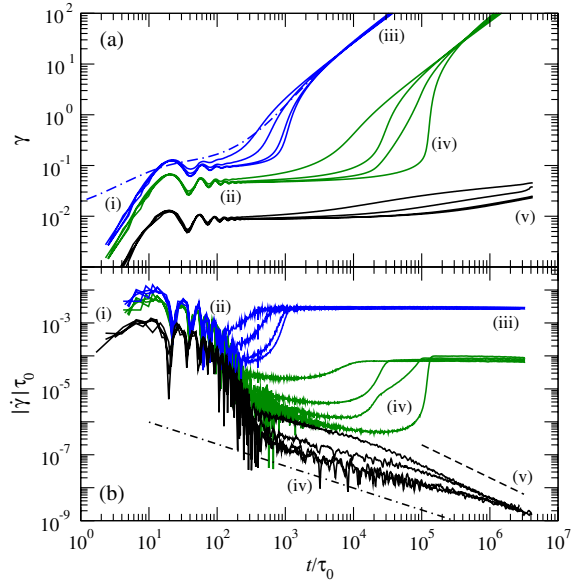
FIG. 4 (color online).   (a) Deformation $\gamma(t)$ for $\sigma/(k_B T/R^3) =$ 0.9, 0.5, and 0.1 (top to bottom, batch B), for waiting times $t_w = 60, 600, 3600,$ and 6000 s (left to right). Dash-dotted: fit used to evaluate $G(t)$, see text. (b) Associated shear rate $\dot{\gamma}(t)$. Dash-dotted line: Andrade creep law, $\dot{\gamma}(t) \sim t^{-2/3}$; dashed: logarithmic creep, $\dot{\gamma}(t) \sim 1/t$.

mode-coupling theory of the glass transition (MCT), $G(t, t') \sim (t - t')^{-a}$ as long as shear-induced relaxation is not dominant [37]. For hard-sphere–like systems, $a \approx 1/3$; inserting this into Eq. (1) yields $\dot{\gamma}(t) \sim t^{-1+a}$, i.e., Andrade's phenomenological law.

In regime (v), $\dot{\gamma}(t)$ is compatible with logarithmic creep, $\dot{\gamma}(t) \sim 1/t$. This has first been suggested in 1905 by Phillips [1] (also called α creep), and is one of the standard creep laws found in hard matter. It is also reported for granular systems [10].

To understand the appearance of logarithmic creep, let us thus assume for $\tau \rightarrow \infty$ a nonlinear generalized Maxwell model, $G(t, t') = G_\infty \exp[-(t - t')\delta\dot{\gamma}(t')/\gamma_c]$. This generalizes a model describing shear thinning by replacing $\tau^{-1} \mapsto \tau^{-1} + \dot{\gamma}/\gamma_c$ [25,38]. It predicts a yield stress $\sigma_c = G_\infty \gamma_c$. Equation (1) then is solved by $\dot{\gamma}(t) = (\tau_{cr}/\tau_0)/t$, under the condition $\sigma = \sigma_c f(\tau_{cr}/\gamma_c\tau_0)$ with $f(x) = xe^x\Gamma(0, x)$. Here Γ denotes the incomplete Gamma function. $f(x)$ increases monotonically and obeys $0 \leq f(x) \leq 1$: logarithmic creep only exists below the yield stress. Approaching σ_c from below ($x \rightarrow \infty$), it shifts to increasingly large time scales [$\tau_{cr} \rightarrow \infty$ as $f(x) \sim 1 - 1/x$], as exhibited by the curves of Fig. 1. While its onset is delayed by aging, both our data and the model suggest the existence of t_w-independent logarithmic creep; in noted difference to SGR [11]. Unlike in studies of gels and pastes [5,7,39], we also find no simple scaling law that collapses curves for different t_w.

The left-hand side of Fig. 2 shows the values of τ_{cr} determined from the data (Fig. 1) together with the

prediction of the generalized Maxwell model (using $G_\infty = 13kT/R^3$ and $\sigma_c = 0.39kT/R^3$). Given that the model is very crude, the agreement with the data is good.

In conclusion we have identified generic laws for the time-dependent creep deformation of a hard-sphere colloidal glass. Below the yield stress ($\sigma < \sigma_c$), Andrade creep ($\dot{\gamma} \sim t^{-x}$) and logarithmic creep ($\dot{\gamma} \sim 1/t$) provide an intriguing connection to the nonlinear deformation behavior of hard-condensed matter, in particular, metallic systems [40]. We find a time scale separating the two power laws that diverges upon the (static) yield stress, as $\tau_{cr}/\tau_0 \sim \gamma_c\sigma_c/(\sigma_c - \sigma)$.

For large stresses, the system is fluidized eventually, on a time scale t_f that diverges with a different power law, connected to the steady-state flow curve. Just before that, the deformation rapidly increases much faster than in viscous flow; this sudden "breaking of the glass" is also known from metallic alloys (tertiary creep, often followed by rupture) [40].

A strong dependence on sample age persists in an intermediate time window at all σ. There appear to be no simple scaling laws accounting for the t_w dependence. We link the mechanisms responsible for the fast breaking and its strong age dependence to the local stress relaxation during cage breaking also observed in the rate-controlled stress-strain curves of noncolloidal and colloidal matter.

The different creep laws are qualitatively explained in terms of the nonlinear Green-Kubo equation (1) and alluding to features of glassy dynamics for the shear modulus $G(t, t'; \dot{\gamma})$. It is a challenge to microscopic theories of glasses, such as MCT under time-dependent flow [14], to recover those relaxation laws. Although we find no reason to assume them, it remains to be explored whether flow-induced heterogeneities affect the dynamics on the microscopic level.

[1] P. Phillips, Philos. Mag., Ser. 6, **9**, 513 (1905).
[2] E. N. da C. Andrade, Proc. R. Soc. A **84**, 1 (1910).
[3] P. Oswald, *Rheophysics* (Cambridge University Press, Cambridge, England, 2009).
[4] R. G. Larson, *The Structure and Rheology of Complex Fluids* (Oxford University Press, Oxford, England, 1998).
[5] M. Cloitre, R. Borrega, and L. Leibler, Phys. Rev. Lett. **85**, 4819 (2000).
[6] P. Coussot, Q. D. Nguyen, H. T. Huynh, and D. Bonn, Phys. Rev. Lett. **88**, 175501 (2002).
[7] A. Negi and C. Osuji, Europhys. Lett. **90**, 28003 (2010).
[8] J. Rosti, J. Koivisto, L. Laurson, and M. J. Alava, Phys. Rev. Lett. **105**, 100601 (2010).
[9] T. Divoux, C. Barentin, and S. Manneville, Soft Matter 7, 8409 (2011).

[10] V. B. Nguyen, T. Darnige, A. Bruand, and E. Clement, Phys. Rev. Lett. **107**, 138303 (2011).

[11] S. M. Fielding, P. Sollich, and M. E. Cates, J. Rheol. **44**, 323 (2000).

[12] C. Derec, A. Ajdari, and F. Lequeux, Eur. Phys. J. E **4**, 355 (2001).

[13] M. Fuchs and M. E. Cates, Phys. Rev. Lett. **89**, 248304 (2002).

[14] J. M. Brader, Th. Voigtmann, M. Fuchs, R. G. Larson, and M. E. Cates, Proc. Natl. Acad. Sci. U.S.A. **106**, 15186 (2009).

[15] R. Besseling, E. R. Weeks, A. B. Schofield, and W. C. K. Poon, Phys. Rev. Lett. **99**, 028301 (2007).

[16] N. Dingenouts, Ch. Norhausen, and M. Ballauff, Macromolecules **31**, 8912 (1998).

[17] M. Siebenbürger, M. Fuchs, H. Winter, and M. Ballauff, J. Rheol. **53**, 707 (2009).

[18] K. N. Pham, G. Petekidis, D. Vlassopoulos, S. U. Egelhaaf, W. C. K. Poon, and P. N. Pusey, J. Rheol. **52**, 649 (2008).

[19] A. Le Grand and G. Petekidis, Rheol. Acta **47**, 579 (2008).

[20] C. Christopoulou, G. Petekidis, B. Erwin, M. Cloitre, and D. Vlassopoulos, Phil. Trans. R. Soc. A **367**, 5051 (2009).

[21] C. Baravian and D. Quemada, Rheol. Acta **37**, 223 (1998).

[22] N. Y. Yao, R. J. Larsen, and D. A. Weitz, J. Rheol. **52**, 1013 (2008).

[23] V. Gopalakrishnan and C. F. Zukoski, J. Rheol. **51**, 623 (2007).

[24] T. Gibaud, D. Frelat, and S. Manneville, Soft Matter **6**, 3482 (2010).

[25] M. Fuchs and M. E. Cates, Faraday Discuss. **123**, 267 (2003).

[26] F. Varnik, L. Bocquet, and J.-L. Barrat, J. Chem. Phys. **120**, 2788 (2004).

[27] D. Hajnal and M. Fuchs, Eur. Phys. J. E **28**, 125 (2009).

[28] A. Fall, J. Paredes, and D. Bonn, Phys. Rev. Lett. **105**, 225502 (2010).

[29] T. Franosch and Th. Voigtmann, J. Stat. Phys. **109**, 237 (2002).

[30] For a completely monotone function $f(x)$ with $f(0) = 1$ there holds $f''(x) - f'(x)f'(0) \geq f''(x) - (f'(x))^2 \geq 0$, as a consequence of Bernstein's theorem.

[31] J. Zausch, J. Horbach, M. Laurati, S. Egelhaaf, J. M. Brader, Th. Voigtmann, and M. Fuchs, J. Phys. Condens. Matter **20**, 404210 (2008).

[32] C. Derec, G. Ducouret, A. Ajdari, and F. Lequeux, Phys. Rev. E **67**, 061403 (2003).

[33] N. Koumakis, M. Laurati, S. U. Egelhaaf, J. F. Brady, and G. Petekidis, Phys. Rev. Lett. **108**, 098303 (2012).

[34] N. F. Mott, Philos. Mag., Ser. 7, **44**, 742 (1953).

[35] M.-C. Miguel, A. Vespignani, M. Zaiser, and S. Zapperi, Phys. Rev. Lett. **89**, 165501 (2002).

[36] T. Bauer, J. Oberdisse, and L. Ramos, Phys. Rev. Lett. **97**, 258303 (2006).

[37] W. Götze, *Complex Dynamics of Glass-Forming Liquids* (Oxford University Press, Oxford, England, 2009).

[38] Th. Voigtmann, Eur. Phys. J. E **34**, 106 (2011).

[39] Y. M. Joshi and G. R. K. Reddy, Phys. Rev. E **77**, 021501 (2008).

[40] D. McLean, Rep. Prog. Phys. **29**, 1 (1966).